Hydrostatic pressure effect on the transport properties in TiO superconducting thin films

X. Liu,[1] C. Zhang,[1] F. X. Hao,[1] T. Y. Wang,[1] Y. J. Fan,[1] Y. W. Yin,[1,*] and X. G. Li[1,2,3,*]

[1]*Hefei National Laboratory for Physical Sciences at the Microscale, Department of Physics, University of Science and Technology of China, Hefei 230026, China*

[2]*Key Laboratory of Materials Physics, Institute of Solid State Physics, CAS, Hefei 230026, China*

[3]*Collaborative Innovation Center of Advanced Microstructures, Nanjing 210093, China*

(Received 14 March 2017; published 5 September 2017)

The superconducting properties of the TiO epitaxial thin films were systematically investigated under hydrostatic pressures (P) up to 2.13 GPa. At ambient pressure, the normal state resistivity increases with decreasing temperature, and steeply increases below $T_{\rm kink} \sim 115$ K. With further reducing temperature to $T_c \sim 5.99$ K, the thin film enters into a superconducting state. Interestingly, the superconducting temperature T_c gradually decreases upon increasing P, and the decreasing rate of T_c with P is much larger than the McMillan theoretical expectation. In contrast, $T_{\rm kink}$ increases with P and a remarkable resistivity enhancement was observed in the temperature range between $T_{\rm kink}$ and T_c. The variations of $T_c, T_{\rm kink}$, and normal state resistivity under high pressure may be induced by the charge localization related to the atomic vacancies rearrangement in TiO thin film. Furthermore, the temperature dependencies of the upper critical field $H_{c2}(T)$ indicate that both the orbital and Pauli-paramagnetic pair-breaking effects should be taken into account. Finally, the thermally activated flux flow investigations under different pressures suggest that the pressure will suppress the thermal activate energy.

DOI: 10.1103/PhysRevB.96.104505

I. INTRODUCTION

Superconducting properties in epitaxial thin films have attracted much attention due to the enhanced or even created superconductivity compared with their bulk forms. For example, the superconducting transition temperature T_c of a $La_{1.9}Sr_{0.1}CuO_4$ thin film (∼49 K) is roughly double of that in the bulk (∼25 K) through epitaxial growth on lattice mismatched $SrLaAlO_4$ substrates [1], and the exotic superconductivity can be created at the $LaAlO_3/SrTiO_3$ interface where a two-dimensional electron gas forms [2–4]. Recently, we succeeded in growing cubic TiO epitaxial thin films on trigonal α-$Al_2O_3(0001)$ single crystalline substrates [5], and found that the zero resistivity temperature $T_c^{\rm zero}$ (∼5.0 K) was much higher than that of the bulk TiO (∼2.8 K) sample [6,7]. However, its mechanism is not clear yet.

Pressure (P) as a basic thermodynamic variable has an important impact on superconductivity. For a superconducting material, a larger dT_c/dP means that a higher T_c may be achieved at ambient pressure through suitable chemical substitution or epitaxial strain design [1,8–10]. More importantly, high pressure experiments benefit to clarify the interplay relationships among various competing orders in superconductors and help to reveal the superconducting mechanisms [11,12]. For example, uniaxial pressure studies in high-T_c cuprates provided evidence that the superconductivity primarily comes from a CuO_2 plane rather than interlayer coupling [13]. In simple s, p metal superconductors like Pb, Sn, In, and Al, it was found that the pressure induced stiffening of the lattice vibration spectrum will lead to a ubiquitous decrease in T_c [14]. While for some metals, such as in thallium and rhenium, the pressure dependencies of T_c are related to the change of the Fermi surface topology and are not monotonous [15], reflecting the complexity of their electronic properties [16].

The pressure effects on the normal state can also present some important information for understanding the mechanisms of superconductivity. In the pressure induced superconductors, such as $BaFe_2S_3$ [17], $1T$-TaS_2 [18], and $2H$-MoS_2 [19], the insulating or semiconducting state at ambient pressure gradually transforms into a metallic state owing to the pressure induced band-gap closure and metallization. While for some other superconductors, such as FeSe [12], $1T$-$TiSe_2$ [20], the structural, electronic, and magnetic transformations in normal state make the pressure dependencies of normal state resistivity exhibit diverse behaviors. Thus, the valuable superconducting information can also be obtained from the evolution of normal state properties with pressure. For example, in the superconductor $LaRu_2P_2$, detailed analysis of the normal state resistivity suggests that the increase of T_c with pressure may be accompanied by an extra electron-boson interaction [21], which results in a much larger enhancement of T_c under hydrostatic pressure than that predicted by McMillan's strong coupling theory. Because the origin of the large enhancement of T_c in TiO thin film is still a mystery [5], the studies on superconducting properties and normal state resistivity under hydrostatic pressures are important to reveal the superconducting mechanism.

In view of these, we have undertaken an extensive study on the superconductivity of TiO thin film under hydrostatic pressures. Temperature dependencies of resistivity from 1.9 to 300 K in different magnetic fields (0–9 T) were measured at various pressures up to 2.13 GPa. Similar to some simple metals, the superconducting transition temperature T_c decreases monotonously with increasing pressure [14]. Furthermore, the temperature dependencies of the upper critical field $H_{c2}(T)$, the irreversibility field $H_{\rm irr}(T)$, and the pair-breaking mechanism were analyzed.

*Corresponding authors: lixg@ustc.edu.cn; yyw@ustc.edu.cn

 ©2017 American Physical Society

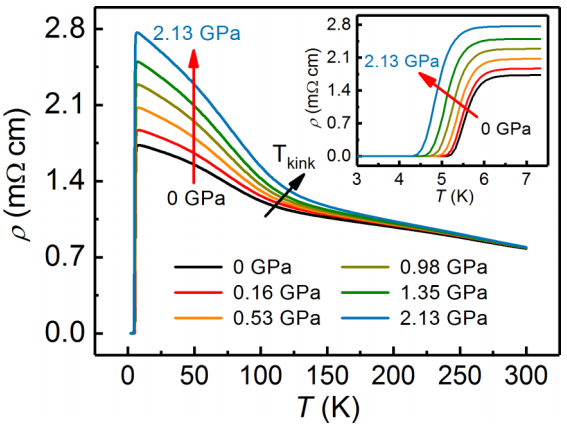

FIG. 1. Temperature dependencies of resistivity (ρ-T) of TiO thin film under various pressures up to 2.13 GPa (0, 0.16, 0.53, 0.98, 1.35, 2.13 GPa). The inset is an enlarged view of the resistivity near T_c.

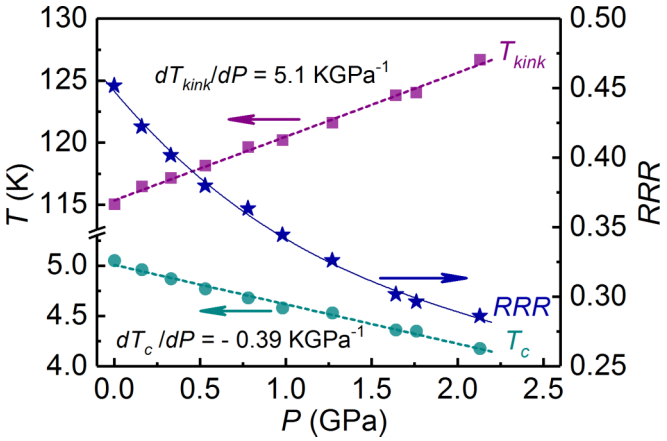

FIG. 2. Pressure dependencies of zero resistive transition temperature T_c (cyan solid circle), kink temperature $T_{\rm kink}$ (purple solid square), and the residual resistivity ratio (RRR) (blue star) of the specimen. The dash lines present the linear fits of T_c and $T_{\rm kink}$ with slopes of -0.39 and 5.1 K GPa^{-1}, respectively. The solid blue line is the eye guide line for RRR.

II. EXPERIMENT

The TiO thin films with a thickness of ~80 nm were epitaxially grown on (0001)-oriented α-Al_2O_3 single crystalline substrates by a pulsed laser deposition technique. A detailed description on the sample preparation and structural characterization was reported in our previous work [5]. The resistivity at different magnetic fields under various pressures was measured by a standard four-probe technique in a Quantum Design Physical Property Measurement System (QD PPMS 9 T). We used a HPC-33 piston type pressure cell to apply hydrostatic pressures on TiO thin films with Daphne 7373 oil as the pressure transmitting medium. The magnitude of pressure was determined by the superconducting transition temperature of Sn in the compressor system. In all measurements, the magnetic fields were applied parallel to the film surface.

III. RESULTS AND DISCUSSION

A. Superconducting transition temperature

Figure 1 presents the temperature (T) dependencies of resistivity (ρ) from 1.9 to 300 K for external pressures up to 2.13 GPa without magnetic field. At ambient pressure, the ρ-T curve exhibits a semiconductorlike behavior at the normal state, where the resistivity increases with decreasing temperature and the residual resistivity ratio ($RRR = \rho_{(300\,\rm K)}/\rho_{\rm max}$) is ~0.45, here $\rho_{\rm max}$ is the maximum resistivity at low temperature. Below the onset superconducting transition temperature $T_c \sim 5.99$ K defined by the resistivity drops to 90% of the normal state resistivity, TiO film enters a superconducting state. Interestingly, a resistivity kink appears around $T_{\rm kink} \sim 115$ K, below which the resistivity increases much steeper. The resistivity kink temperature $T_{\rm kink}$, related to an electronic property change [22,23], was defined as the cross point of the fittings below and above the $T_{\rm kink}$ [for the details, please see Fig. 3(a)]. It is known that there is an energy gap of 0.06–0.17 eV between the valence and the conduction bands in TiO_x($x \geqslant 1.087$) with disordered vacancies [24], which is of the same order of magnitude as the pseudogap near the Fermi level calculated from the first-principle theory [25]. Therefore, the semiconductorlike temperature dependencies of resistivity in the normal state of our TiO film may be related to the gap and impacted by the atom vacancies and disorders [26].

The normal state resistivity increases with increasing pressure P, and it becomes more remarkable below $T_{\rm kink}$ than above $T_{\rm kink}$. The top inset of Fig. 1 is an enlarged view of the ρ-T curves near T_c and it is clear that T_c drops gradually with increasing P. These behaviors are different from most conventional BCS simple metal superconductors, in which the decrease of T_c under pressure usually accompanies the decrease of normal state resistivity due to the weakening of electron-phonon coupling under pressures [14]. Figure 2 shows that the variations of T_c, $T_{\rm kink}$, and RRR with P, T_c, and $T_{\rm kink}$ follow linear dependencies with $dT_c/dP = -0.39$ K GPa^{-1} and $dT_{\rm kink}/dP = 5.1$ K GPa^{-1}, respectively. While the RRR decreases with increasing P and exhibits a concave shape. Considering that T_c is closely related to the electron-phonon interaction while $T_{\rm kink}$ is mainly due to the electronic property change [22,23], the opposite pressure evolution tendency between T_c and $T_{\rm kink}$ suggests that the changes of electronic properties in normal state suppress the superconductivity in TiO thin film by competing with electron-phonon interaction.

The pressure dependencies of T_c are analyzed within the framework of McMillan theory as follows [27]:

$$T_c = \frac{\Theta_D}{1.45} \exp\left\{\frac{-1.04(1+\lambda)}{\lambda - \mu^*(1+0.62\lambda)}\right\}. \quad (1)$$

Here T_c is related to the fundamental parameters including the electron-phonon coupling parameter λ, the Coulomb repulsion μ^*, and the Debye temperature Θ_D. In most BCS superconductors μ^* equals a value of 0.1 [16,28,29], and the change of μ^* with pressure can be neglected [16]. Formula (1) has been successfully used in a number of superconducting materials in deriving T_c under pressures, such as elemental superconductors [30], transition-metal nitrides [31], MgB_2

[32,33], H_3S [34], NbO [29], and so on. Taking the logarithmic volume derivative of T_c in Eq. (1), one can obtain the following relation [28]:

$$\frac{d\ln T_c}{d\ln V} = -B\frac{d\ln T_c}{dP} = -\gamma + \Delta\left\{\frac{d\ln\eta}{d\ln V} + 2\gamma\right\}, \quad (2)$$

where $\gamma = -d\ln\langle\omega\rangle/d\ln V$ is the Grüneisen parameter, $\eta = N(E_F)\langle I^2\rangle$ is the Hopfield parameter, $N(E_F)$ is the density of states at the Fermi level, $\langle I^2\rangle$ is the average square electronic matrix element, and $\Delta = 1.04\lambda[1+0.38\mu^*][\lambda-\mu^*(1+0.62\lambda)]^{-2}$ [35]. The applied pressure will be converted to a volume change using the bulk modulus parameter B, as the volume directly correlates with the lattice vibrational frequency through the fundamental parameter γ. The terms of $d\ln\eta/d\ln V$ and $\gamma = -d\ln\langle\omega\rangle/d\ln V$ in Eq. (2) represent the changes of electronic and lattice properties with volume, respectively. The typical $d\ln\eta/d\ln V$ equals -1 for simple s and p metal superconductors [36], -3 to -4 for d-band superconducting transition metal [35], and -1 to -4 for compound superconductors [28,31], respectively.

Using zero resistivity superconducting transition temperature $T_c^{zero} = 5$ K at ambient pressure, $\Theta_D = 560$ K [29], and $\mu^* = 0.1$ [16,28,29], we obtained $\lambda = 0.486$ and $\Delta = 4.14$ from Eq. (1). Inserting these values into Eq. (2) and setting $\gamma = 1.2$ [37] and $B_{TiO} = 260$ GPa [25], we have $dT_c/dP = -0.09$–0.15 K GPa^{-1} with $d\ln\eta/d\ln V = -1$ to -4 (if the α-Al_2O_3 bulk modulus B of about 250 GPa is used [38], then dT_c/dP is about -0.09–0.16 K GPa^{-1}). The experimental reduction of T_c with pressure ($dT_c/dP = -0.39$ K GPa^{-1}) is much stronger than the theoretical prediction. This suggests that the decrease of T_c in TiO film cannot be simply interpreted by the basic change of electron-phonon interaction under pressure.

In order to get a deeper insight of the pressure weakened superconductivity, we took a close look at the normal state resistivity under pressures. For the TiO film, the semiconductorlike behavior of the ρ-T curves in a certain temperature range below and above T_{kink} follows the variable range hopping (VRH) relation [39]:

$$\rho(T) = \rho_0\exp(T_0/T)^{1/4}. \quad (3)$$

Here ρ_0 is a constant, and the characteristic temperature T_0 is given by

$$T_0 = 24/\left[\pi k_B N(E_F)\xi_l^3\right], \quad (4)$$

where ξ_l is the localization length. The fitting results under various pressures are shown in Fig. 3(a). In ambient pressure, the ρ-T curve could be described over two distinct regions, 115–190 K (above T_{kink} defined as the cross point of the linear fittings) and 75–115 K (below T_{kink}), with $T_0 = 246$ and 857 K in both regions, respectively. As illustrated in Fig. 3(b), T_0 values for both regions were found to increase with increasing P, indicating the decrease of $N(E_F)\xi_l^3$. Some calculations presented that the $N(E_F)$ value roughly doubled when the atom vacancies changed from a complete ordering to complete disordering state [25,26], however, the T_0 increases by more than one order of magnitude below T_{kink}. Therefore, we believe that the decrease of ξ_l and enhancement of charge localization would be the main reasons for the increase of T_0. The rapid increase of T_0 below T_{kink} suggests that a hydrostatic pressure

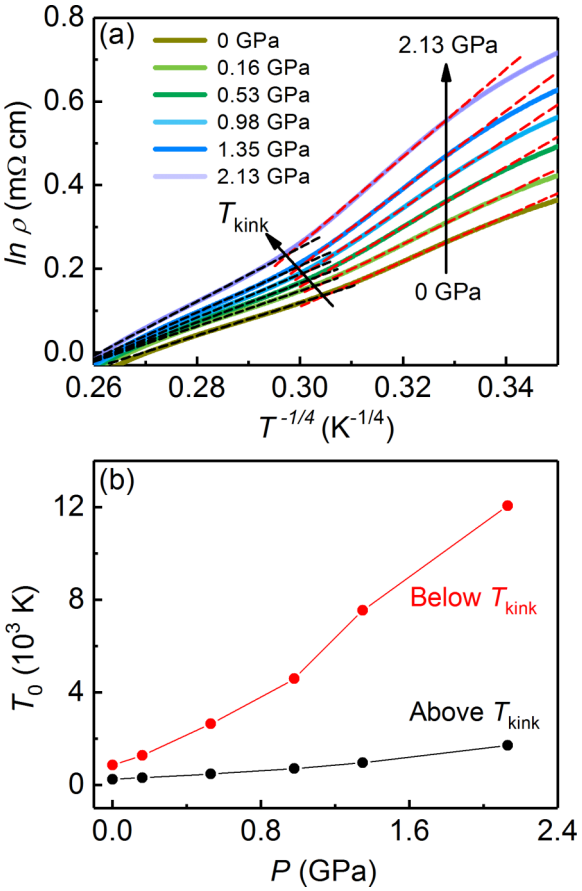

FIG. 3. (a) Fits of resistivity data with variable range hopping model at various pressures (0, 0.16, 0.53, 0.98, 1.35, and 2.13 GPa). (b) Characteristic temperatures at temperatures above T_{kink} (black) and below T_{kink} (red) plotted as a function of pressure.

will significantly enhance the charge localization below T_{kink}. Such a resistivity kink was also observed in Ti_3O_5 and Ti_4O_7 superconducting thin films [40], which were attributed to a bipolaronic interaction. But we should note that the bipolaronic transition temperature could be reduced under pressure [22,41], and the increasing T_{kink} in our TiO thin films contradicts with that predicted by the bipolaronic model [22,40,41].

Because the carrier localization will suppress the formation of Cooper pairs [42], the pressure induced enhancement of carrier localization should unavoidably reduce the T_c significantly, leading to a much larger dT_c/dP than the calculation by McMillan theory. It is known that atomic titanium and oxygen vacancies are the typical characteristic in a TiO system and often form a superstructure with ordered atomic vacancies [43]. Different physical properties can be obtained by varying the number and arrangement of vacancies in the TiO crystal structure [44]. It was demonstrated that the application of pressure will affect the arrangement of vacancies in TiO_x powder [45]. Similarly, the high pressure applied on the TiO thin film will induce atomic vacancies rearrangement as well, and affect the local chemical environments and electronic structures accordingly, which may be the reason of the enhancement of carrier localization.

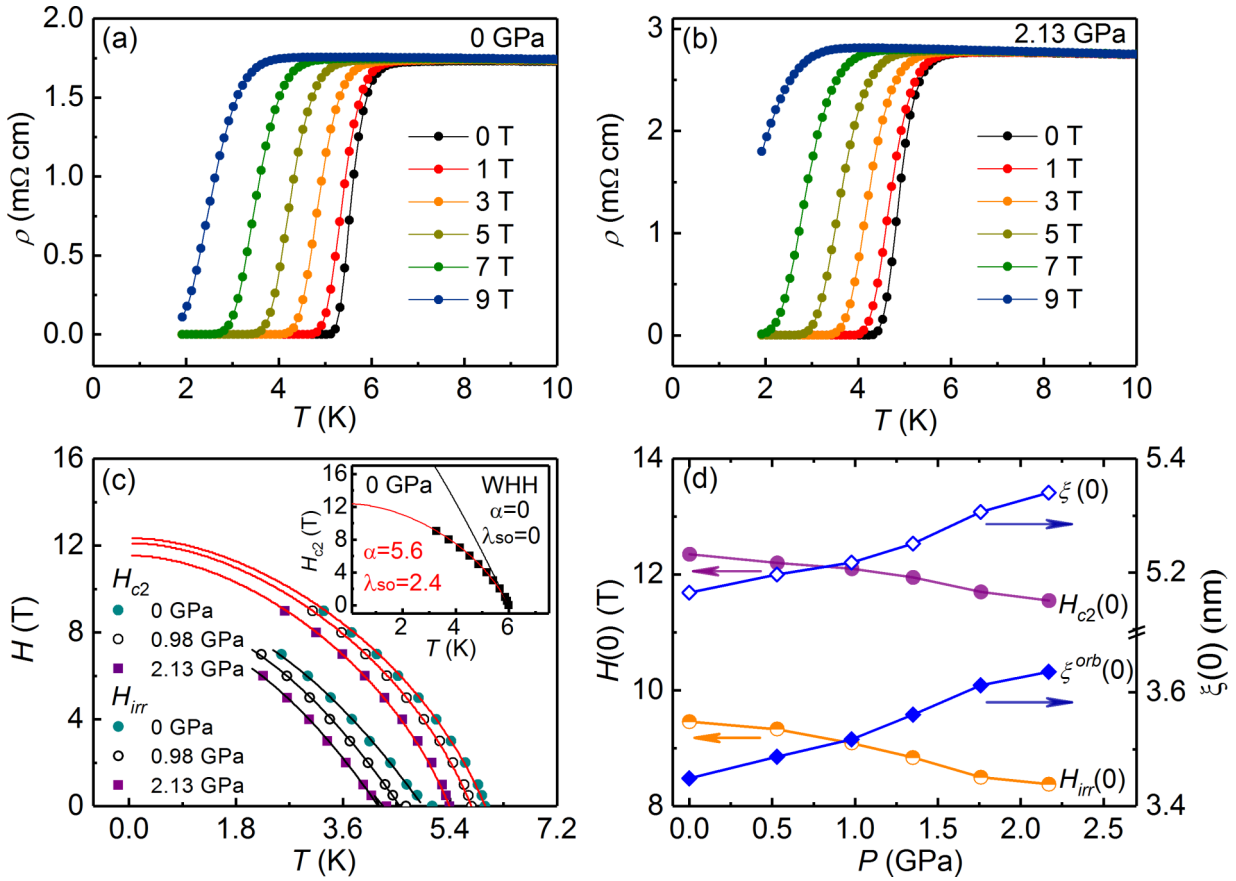

FIG. 4. (a) and (b) ρ-T curves for TiO thin film in different magnetic fields under the selected pressures of 0 and 2.13 GPa. (c) $H_{c2}(T)$ and $H_{\rm irr}(T)$ as a function of temperature at the representative pressures, the red lines are the fits to the WHH model with consideration of the spin-paramagnetic and the spin-orbit effects (0, 0.98, and 2.13 GPa), and the black lines are the fits to the empirical equation $H_{\rm irr}(T) = H_{\rm irr}(0)[1-(T/T_c)^2]$ (0, 0.98, and 2.13 GPa). Inset: Analysis of $H_{c2}(T)$ (0 GPa) using the WHH theory without (black line) and with (red line) spin-paramagnetic effect and spin orbital scattering. (d) Pressure dependencies of $H_{c2}(0), H_{\rm irr}(0)$, $\xi^{\rm orb}(0)$, and $\xi(0)$.

Although we qualitatively or semiquantitatively analyzed the variations of T_c with pressures, more accurate analysis of pressure dependence of T_c needs a definite $\eta = N(E_{\rm F})\langle I^2\rangle$ which can be calculated by electronic-structure theory [46] or measured through phonon spectra [47]. Moreover, the lack of experimental studies for pressure effects on atomic vacancies makes it more mysterious. These aspects deserve further investigation.

B. Upper critical field

Now, let us analyze the pressure effect on the upper critical field H_{c2} which provides valuable information on fundamental superconducting properties, such as the coherence length and the pair-breaking mechanism. We measured the superconducting transition broadening behaviors in magnetic fields with different pressures. Figures 4(a) and 4(b) show the temperature dependencies of resistivity in different magnetic fields at the selected pressures of 0 and 2.13 GPa. Similar broadenings of the superconducting transition were also obtained under other pressures. The temperature dependencies of the upper critical fields $H_{c2}(T)$ defined by the resistivity drops to 90% of the normal state resistivity are shown in the Fig. 4(c). The H_{c2} versus temperature curves in all pressures exhibit a convex shape and the initial slope $dH_{c2}/dT|_{T=T_c}$ is about -6.7T K^{-1}.

As we know, the variation of H_{c2} with temperature is closely related to the pair-breaking mechanism. Generally, the Cooper pair can be destroyed via the orbital pair-breaking effect and the Pauli-paramagnetic (spin-paramagnetic) pair-breaking effect in external magnetic fields. The former is rising from the Lorentz force acting on paired electrons, while the later originates from the Zeeman effect. Considering the contributions of each pair-breaking mechanism, the temperature dependencies of $H_{c2}(T)$ can be calculated using Werthamer-Helfand-Hohenberg (WHH) theory which is given by [48]

$$\ln\frac{1}{t} = \left(\frac{1}{2}+\frac{i\lambda_{\rm so}}{4\gamma}\right)\psi\left(\frac{1}{2}+\frac{\overline{h}+\lambda_{\rm so}/2+i\gamma}{2t}\right) + \left(\frac{1}{2}-\frac{i\lambda_{\rm so}}{4\gamma}\right)\psi\left(\frac{1}{2}+\frac{\overline{h}+\lambda_{\rm so}/2-i\gamma}{2t}\right)-\psi\left(\frac{1}{2}\right), \tag{5}$$

here $t = T/T_c$, $\overline{h} = \frac{4H_{c2}}{\pi^2(-dH_{c2}/dt)_{t=1}}$, $\gamma = [(\alpha\overline{h})^2 - (\lambda_{\rm so}/2)^2]^{1/2}$, α is the Maki parameter representing the relative strength of spin and orbital pair breakings, and $\lambda_{\rm so}$ is the spin-orbit scattering constant. Equation (5) fits the experimental data very well with the fitting parameters $\alpha = 5.6, \lambda_{\rm so} = 2.4$, and $H_{c2}(0) = 12.35$ T, as shown in Fig. 4(c). It should be noted that if the orbital effect is dominant ($\alpha = 0$) and the spin-orbit

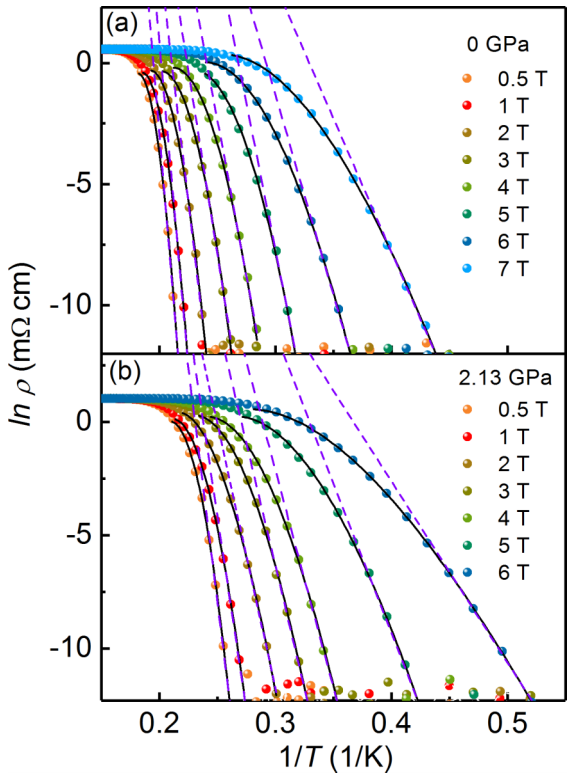

FIG. 5. lnρ vs $1/T$ curves at (a) 0 GPa and (b) 2.13 GPa. The black solid lines are the regressive curves obtained using a modified TAFF method, and the purple dashed lines show a linear Arrhenius relation fitting for the resistivity broadenings.

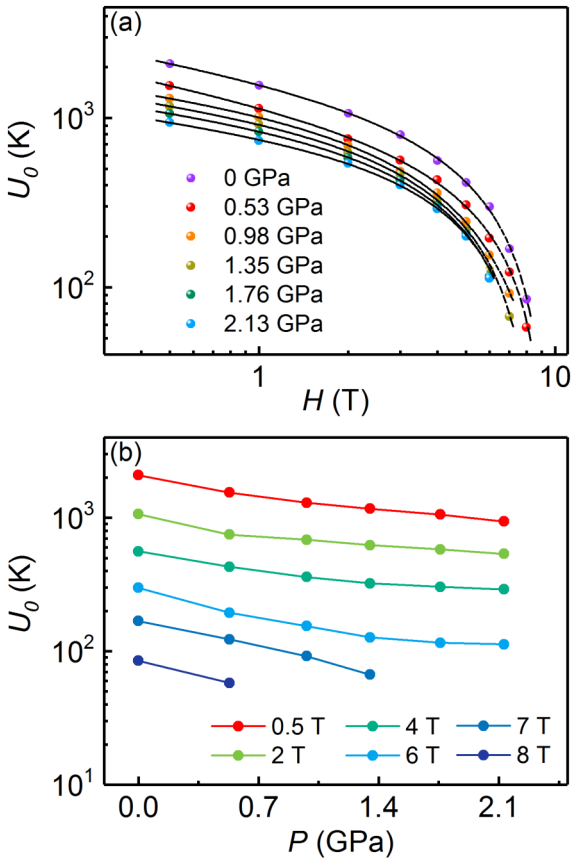

FIG. 6. (a) U_0 as a function of magnetic fields obtained by fitting the resistivity in TAFF region using the modified TAFF model. The black dash lines are the fittings using Eq. (7). (b) Pressure dependencies of U_0 in various magnetic fields.

scattering is negligible ($\lambda_{so} = 0$), we got the orbital limited upper critical field $H_{c2}^{orb}(0) = -0.69T_c dH_{c2}/dT|_{T=T_c} = 27.7$ T at ambient pressure, as plotted in the inset of Fig. 4(c). While for the Pauli-paramagnetic effect, the Pauli-paramagnetic limiting field is obtained from $H_{c2}^{P}(0) = \sqrt{2}H_{c2}^{orb}(0)/\alpha = 7.0$ T [49]. Comparing the values of $H_{c2}(0)$, $H_{c2}^{orb}(0)$, and $H_{c2}^{P}(0)$, we can see that both the orbital and Pauli-paramagnetic pair-breaking effects should be taken into account. The same analysis was applied to the $H_{c2}(T)$ at various pressures, and we found that $H_{c2}(0)$ decreases from 12.35 to 11.55 T with increasing pressures from 0 to 2.13 GPa. The superconducting coherence length $\xi(0)$ at absolute zero temperature could be estimated by Ginzburg-Landau formula $\xi(0) = [\varphi_0/2\pi H_{c2}(0)]^{1/2}$, where $\varphi_0 = 2.07 \times 10^{-15}$ Wb is the flux quantum. One may use the orbital-limiting field $H_{c2}^{orb}(0)$ [50,51], the fitted upper critical field $H_{c2}(0)$ [52,53], or the Pauli-paramagnetic limiting field $H_{c2}^{P}(0)$ [52,54] to estimate the coherence length even though there is a large difference between $H_{c2}^{orb}(0)$ and $H_{c2}(0)$. For TiO thin films, $\xi^{orb}(0)$ and $\xi(0)$ were calculated using $H_{c2}^{orb}(0)$ and $H_{c2}(0)$, respectively, and both of the coherence lengths increase with increasing pressure, as shown in Fig. 4(d).

C. Flux pinning

From the broadening of resistive transition of TiO thin films, the behaviors of flux flow and the thermally activated energy can be obtained. Figure 4(c) shows the pressure effect on the temperature dependencies of the irreversibility fields $H_{irr}(T)$ defined by the resistivity drops to 0.1% of the normal state resistivity. The variations of $H_{irr}(T)$ with temperature under different pressures can be well fitted by an empirical equation $H_{irr}(T) = H_{irr}(0)[1 - (T/T_c)^2]$, where $H_{irr}(0)$ is the irreversibility field at absolute zero temperature. Similar to $H_{c2}(T)$, the value of $H_{irr}(0)$ is suppressed by the hydrostatic pressures as displayed in Fig. 4(d).

Furthermore, according to a modified thermally activated flux flow (TAFF) theory, the TAFF resistivity is expressed as [55]

$$\ln\rho = \ln[2\rho_c U_0(H)] + q\ln(1-t) - \ln T - U_0(H)(1-t)^q/T, \quad (6)$$

where q and ρ_c are the temperature independent parameters, $U_0(H)$ is the thermally activated energy for flux flow, and $t = T/T_c(H)$. We found that $q = 2$ is in good agreement with experimental data, shown as solid black lines in Figs. 5(a) and 5(b). Simple TAFF fittings with Arrhenius relation are also displayed as the dashed purple lines in Fig. 5, which cannot fit the entire region of the given data, similar to the that in $Nb(N_{0.98}O_{0.02})$ [56].

Figure 6(a) shows that the magnetic field dependence of $U_0(H)$ obtained from the fittings using Eq. (6) at various

pressures obeys the following phenomenological formula [56]:

$$U_0(H) \propto H^{-\gamma}\left(1-\frac{H}{H_{\rm irr}}\right)^{\delta}, \quad (7)$$

where γ and δ are fitting parameters, in the range of 0.22–0.35, and 1.22–1.45, respectively, as shown in Fig. 6(a) by dash lines. Upon increasing pressure, U_0 shows a downward trend as plotted in the Fig. 6(b).

IV. CONCLUSIONS

In summary, we systematically studied the superconducting properties of TiO epitaxial thin films under hydrostatic pressures up to 2.13 GPa. With increasing P, T_c gradually decreases while normal state resistivity and its anomaly temperature $T_{\rm kink}$ increase. A quantified analysis of pressure dependent T_c demonstrated that the value of T_c decreases much quicker than McMillan's theoretical expectation. The analysis of normal state resistivity showed that the ρ-T behaviors can be explained by variable range hopping mechanism, and the carrier localization in TiO thin film is significantly enhanced by pressure especially below $T_{\rm kink}$. The carrier localization in high pressure was considered to be the reason for the variations of T_c and $T_{\rm kink}$, which may be caused by the atom vacancy rearrangement under pressure. The analysis of temperature dependencies of $H_{c2}(T)$ revealed that both the orbital and Pauli-paramagnetic pair-breaking effects should be taken into account. In addition, it was found that the pressure can suppress the thermal activate energy for flux motion.

ACKNOWLEDGMENT

This work was supported by the National Natural Science Foundation of China (Grants No. 51332007, No. 21521001, and No. 51622209) and by the National Basic Research Program of China (Grants No. 2016YFA0300103, No. 2015CB921201, and No. 2012CB922003).

[1] J.-P. Locquet, J. Perret, J. Fompeyrine, E. Mächler, J. W. Seo, and G. Van Tendeloo, Nature (London) **394**, 453 (1998).
[2] L. Li, C. Richter, J. Mannhart, and R. C. Ashoori, Nat. Phys. **7**, 762 (2011).
[3] J. A. Bert, B. Kalisky, C. Bell, M. Kim, Y. Hikita, H. Y. Hwang, and K. A. Moler, Nat. Phys. **7**, 767 (2011).
[4] C. Richter, H. Boschker, W. Dietsche, E. Fillis-Tsirakis, R. Jany, F. Loder, L. F. Kourkoutis, D. A. Muller, J. R. Kirtley, C. W. Schneider, and J. Mannhart, Nature (London) **502**, 528 (2013).
[5] C. Zhang, F. X. Hao, G. Y. Gao, X. Liu, C. Ma, Y. Lin, Y. W. Yin, and X. G. Li, npj Quantum Mater. **2**, 2 (2017).
[6] J. K. Hulm, C. K. Jones, R. A. Hein, and J. W. Gibson, J. Low Temp. Phys. **7**, 291 (1972).
[7] D. Wang, C. Huang, J. He, X. Che, H. Zhang, and F. Huang, ACS Omega **2**, 1036 (2017).
[8] X. H. Chen, T. Wu, G. Wu, R. H. Liu, H. Chen, and D. F. Fang, Nature (London) **453**, 761 (2008).
[9] K. Iida, V. Grinenko, F. Kurth, A. Ichinose, I. Tsukada, E. Ahrens, A. Pukenas, P. Chekhonin, W. Skrotzki, A. Teresiak, R. Hühne, S. Aswartham, S. Wurmehl, I. Mönch, M. Erbe, J. Hänisch, B. Holzapfel, S. L. Drechsler, and D. V. Efremov, Sci. Rep. **6**, 28390 (2016).
[10] Y. Mizuguchi, Y. Hara, K. Deguchi, S. Tsuda, T. Yamaguchi, K. Takeda, H. Kotegawa, H. Tou, and Y. Takano, Supercond. Sci. Technol. **23**, 054013 (2010).
[11] K. Kothapalli, A. E. Böhmer, W. T. Jayasekara, B. G. Ueland, P. Das, A. Sapkota, V. Taufour, Y. Xiao, E. Alp, S. L. Bud'ko, P. C. Canfield, A. Kreyssig, and A. I. Goldman, Nat. Commun. **7**, 12728 (2016).
[12] J. P. Sun, K. Matsuura, G. Z. Ye, Y. Mizukami, M. Shimozawa, K. Matsubayashi, M. Yamashita, T. Watashige, S. Kasahara, Y. Matsuda, J.-Q. Yan, B. C. Sales, Y. Uwatoko, J.-G. Cheng, and T. Shibauchi, Nat. Commun. **7**, 12146 (2016).
[13] F. Gugenberger, C. Meingast, G. Roth, K. Grube, V. Breit, T. Weber, H. Wühl, S. Uchida, and Y. Nakamura, Phys. Rev. B **49**, 13137 (1994).
[14] P. E. Seiden, Phys. Rev. **179**, 458 (1969).
[15] C. W. Chu, T. F. Smith, and W. E. Gardner, Phys. Rev. Lett. **20**, 198 (1968).
[16] J. R. Schrieffer and J. S. Brooks, *Handbook of High-Temperature Superconductivity Theory and Experiment* (Springer, Berlin, 2007).
[17] T. Yamauchi, Y. Hirata, Y. Ueda, and K. Ohgushi, Phys. Rev. Lett. **115**, 246402 (2015).
[18] B. Sipos, A. F. Kusmartseva, A. Akrap, H. Berger, L. Forró, and E. Tutiš, Nat. Mater. **7**, 960 (2008).
[19] Z. Chi, F. Yen, F. Peng, J. Zhu, Y. Zhang, X. Chen, Z. Yang, X. Liu, Y. Ma, Y. Zhao, T. Kagayama, and Y. Iwasa, arXiv:1503.05331.
[20] A. F. Kusmartseva, B. Sipos, H. Berger, L. Forró, and E. Tutiš, Phys. Rev. Lett. **103**, 236401 (2009).
[21] B. X. Li, P. C. Lu, J. Z. Liu, J. Sun, S. Li, X. Y. Zhu, and H.-H. Wen, Sci. Rep. **6**, 24479 (2016).
[22] H. Ueda, K. Kitazawa, H. Takagi, and T. Matsumoto, J. Phys. Soc. Jpn. **71**, 1506 (2002).
[23] M. Marezio, D. B. McWhan, P. D. Dernier, and J. P. Remeika, Phys. Rev. Lett. **28**, 1390 (1972).
[24] A. A. Valeeva, A. A. Rempel', and A. I. Gusev, JETP Lett. **73**, 621 (2001).
[25] D. A. Andersson, P. A. Korzhavyi, and B. Johansson, Phys. Rev. B **71**, 144101 (2005).
[26] M. G. Kostenko, A. V. Lukoyanov, V. P. Zhukov, and A. A. Rempel, JETP Lett. **95**, 647 (2012).
[27] W. L. McMillan, Phys. Rev. **167**, 331 (1968).
[28] T. Tomita, J. J. Hamlin, J. S. Schilling, D. G. Hinks, and J. D. Jorgensen, Phys. Rev. B **64**, 092505 (2001).
[29] A. M. Okaz and P. H. Keesom, Phys. Rev. B **12**, 4917 (1975).
[30] J. L. Olsen, K. Andres, and T. H. Geballe, Phys. Lett. A **26**, 239 (1968).
[31] X. J. Chen, V. V. Struzhkin, S. Kung, H.-K. Mao, R. J. Hemley, and A. N. Christensen, Phys. Rev. B **70**, 014501 (2004).
[32] X. J. Chen, H. Zhang, and H.-U. Habermeier, Phys. Rev. B **65**, 144514 (2002).
[33] J.-C. Zheng and Y. Zhu, Phys. Rev. B **73**, 024509 (2006).

[34] D. Duan, Y. Liu, F. Tian, D. Li, X. Huang, Z. Zhao, H. Yu, B. Liu, W. Tian, and T. Cui, Sci. Rep. **4**, 6968 (2014).
[35] J. J. Hopfield, Physica **55**, 41 (1971).
[36] A. Eiling and J. S. Schilling, J. Phys. F: Met. Phys. **11**, 623 (1981).
[37] A. Taylor and N. J. Doyle, J. Appl. Crystallogr. **4**, 109 (1971).
[38] B. Holm, R. Ahuja, Y. Yourdshahyan, B. Johansson, and B. I. Lundqvist, Phys. Rev. B **59**, 12777 (1999).
[39] L. Zhang and Z.-J. Tang, Phys. Rev. B **70**, 174306 (2004).
[40] K. Yoshimatsu, O. Sakata, and A. Ohtomo, arXiv:1612.02502.
[41] T. Tonogai, H. Takagi, C. Murayama, and N. Môri, Rev. High Pressure Sci. Technol. **7**, 453 (1998).
[42] B. Sacépé, T. Dubouchet, C. Chapelier, M. Sanquer, M. Ovadia, D. Shahar, M. Feigel'man, and L. Ioffe, Nat. Phys. **7**, 239 (2011).
[43] A. A. Valeeva, A. A. Rempel, W. Sprengel, and H.-E. Schaefer, Phys. Rev. B **75**, 094107 (2007).
[44] A. I. Gusev, A. A. Rempel, and A. J. Magerl, *Disorder and Order in Strongly Nonstoichiometric Compounds: Transition Metal Carbides, Nitrides and Oxides* (Springer, Berlin, 2013).
[45] T. Fujimura, H. Iwasaki, T. Kkegawa, Y. Tsuchida, O. Terasaki, and O. Shimomura, High Press. Res. **1**, 213 (1989).
[46] R. Evans, V. K. Ratti, and B. L. Gyorffy, J. Phys. F: Met. Phys. **3**, L199 (1973).
[47] X. J. Chen, V. V. Struzhkin, Z. Wu, R. E. Cohen, S. Kung, H.-K. Mao, R. J. Hemley, and A. N. Christensen, Phys. Rev. B **72**, 094514 (2005).
[48] N. R. Werthamer, E. Helfand, and P. C. Hohenberg, Phys. Rev. **147**, 295 (1966).
[49] H. C. Lei, R. W. Hu, E. S. Choi, J. B. Warren, and C. Petrovic, Phys. Rev. B **81**, 094518 (2010).
[50] V. A. Gasparov, A. Audouard, L. Drigo, A. I. Rodigin, C. T. Lin, W. P. Liu, M. Zhang, A. F. Wang, X. H. Chen, H. S. Jeevan, J. Maiwald, and P. Gegenwart, Phys. Rev. B **87**, 094508 (2013).
[51] S. Khim, B. Lee, J. W. Kim, E. S. Choi, G. R. Stewart, and K. H. Kim, Phys. Rev. B **84**, 104502 (2011).
[52] X. Xing, W. Zhou, J. Wang, Z. Zhu, Y. Zhang, N. Zhou, B. Qian, X. Xu, and Z. Shi, Sci. Rep. **7**, 45943 (2017).
[53] H. C. Lei, R. W. Hu, E. S. Choi, J. B. Warren, and C. Petrovic, Phys. Rev. B **81**, 184522 (2010).
[54] K. Wang, H. Ryu, E. Kampert, M. Uhlarz, J. Warren, J. Wosnitza, and C. Petrovic, Phys. Rev. X **4**, 031018 (2014).
[55] H. C. Lei, K. F. Wang, R. W. Hu, H. Ryu, M. Abeykoon, E. S. Bozin, and C. Petrovic, Sci. Technol. Adv. Mat. **13**, 054305 (2012).
[56] D. Venkateshwarlu, V. Ganesan, Y. Ohashi, S. Kikkawa, and J. V. Yakhmi, Supercond. Sci. Tech. **28**, 055009 (2015).